Printed in the Republic of Korea

ANALYTICAL SCIENCE & TECHNOLOGY

Vol. 39 No. 1, 1-12, 2026

https://doi.org/10.5806/AST.2026.39.1.1

Forensic interpretation of evaporatively weathered kerosene–diesel mixtures using UCM-based gas chromatographic profiling

Sookyung Jeon★ and Gum mun Nam

Forensic Toxicology & Chemistry, Gwangju Institute, National Forensic Service, Jangseong Gun, 57248, Republic of Korea

(Received September 4, 2025; Revised November 23, 2025; Accepted January 9, 2026)

Abstract: Petroleum fuels such as kerosene and diesel are important forensic indicators in investigations of fires, explosions, and oil spill incidents. However, environmental exposure can alter their chemical composition through weathering, particularly evaporation, complicating mixture identification and source tracking. In this study, we quantified the unresolved complex mixture (UCM) region in gas chromatography (GC) chromatograms to describe compositional changes in kerosene–diesel mixtures during short-term evaporative weathering and to assess its utility for mixture identification. Artificially contaminated soil samples with various mixing ratios were prepared and subjected to controlled evaporation for up to 90 days. Samples were collected at regular intervals, and the area and distribution characteristics of the UCM region were compared. The results showed that kerosene components evaporated faster than diesel components, and over time the mixtures could appear as a single fuel type when interpreted primarily from major peaks. In contrast, UCM distribution features and area-based indicators differed with the initial mixing ratio, suggesting that UCM analysis can provide clues to mixture presence and initial composition even when peak-based interpretation is ambiguous. Overall, UCM-based GC profiling may complement conventional compound- and peak-centered interpretation and provides foundational data for future validation under broader conditions.

Keywords: evaporative weathering, kerosene–diesel mixture, unresolved complex mixture (UCM), gas chromatography (GC), forensic interpretation

1. Introduction

The analysis of flammable petroleum products such as gasoline, kerosene, diesel, and heavy oil in fire incidents, accidents, marine oil spills, and explosions serves as a critical means of determining the cause of the event and assessing the possibility of criminal involvement. Such analyses also provide valuable insights into the physicochemical characteristics of combustion events, thereby enabling forensic reconstruction of the sequence of events that transpired.[1-5]

Gasoline, kerosene, diesel, and lubricants are all petroleum-derived mixtures produced during the fractional distillation of crude oil, primarily separated

★ Corresponding author
Phone : +82-(0)61-399-3671 Fax : +82-(0)61-399-3679
E-mail : neon152@korea.kr

according to differences in boiling-point ranges (i.e., naphtha, middle distillates, and residual fractions).[6,7] These fuels contain hundreds of hydrocarbons, each exhibiting characteristic chromatographic patterns in gas chromatography (GC). Gasoline and lubricants typically produce distinct chromatographic profiles, whereas kerosene and diesel share a substantial number of overlapping components. Kerosene generally contains hydrocarbons ranging from nonane (C_9) to hexadecane (C_{16}), while diesel spans a broader range from decane (C_{10}) to tricosane (C_{23}).[2,7−10] In the absence of evaporative weathering or mixing, the chromatogram of each fuel is sufficient for unambiguous identification. However, once petroleum mixtures are released into the environment, weathering processes—including dissolution, evaporation, photo-oxidation, and biodegradation—modify their chemical composition and increase chromatographic complexity, thereby complicating forensic and environmental interpretation.[1,11] Recent studies have emphasized the importance of robust sample-preparation methodologies and advanced hydrocarbon-profiling strategies for accurately characterizing complex petroleum-based matrices, particularly weathered oils and contaminated soils where quantitative information is essential for environmental and forensic assessments.[12]

In the event of oil spillage into the environment, the components observed during weathering (dissolution, evaporation, photo-oxidation, and biodegradation) differ from the original substance.[3,6,11] A variety of analytical techniques are employed for the analysis of oil, with gas chromatography (GC)-based equipment being a widely utilized example. A visual comparison of the chromatogram is made to either a reference chromatogram of a known standard (i.e., pattern matching) or to a mass spectrum library database.[2,13] Gas chromatography-mass spectrometry (GC-MS) is a widely used analytical technique to characterize the composition of oil samples. This analytical method is particularly useful in the identification and differentiation of components in diverse oil types, including those that are mixed or have undergone weathering. Particularly, analysis using weathering-resistant petroleum biomarkers, such as steranes, hopanes, and polycyclic aromatic hydrocarbons (PAHs), is being used effectively to trace the source of contamination in weathered samples.[3,14] However, distinguishing fuels with overlapping components (e.g., kerosene and diesel) remains challenging when relying solely on traditional peak-based interpretation. These limitations underscore the need for complementary analytical approaches capable of quantitatively assessing the weathering of blended fuels.

The Unresolved Complex Mixture (UCM), observed as a broad, elevated hump in GC chromatograms, represents thousands of co-eluting hydrocarbons—including alkanes, aromatics, cycloalkanes, heteroatomic species, steranes, and triterpenoids.[14-19] UCM characteristics vary according to fuel type, and previous studies have shown that parameters such as the time of maximum intensity (T_{UCM}) and hump width (w) can be used to differentiate petroleum products in contaminated soils.[20-22] Importantly, these indicators remain distinguishable even after partial environmental weathering. Earlier studies combining GC–MS with UCM analysis have indicated the utility of UCM-based metrics for identifying petroleum pollution sources.[23] However, most prior work has focused on single-fuel systems, and quantitative interpretation of UCM behavior in blended fuels subjected to evaporation-driven weathering remains limited. Recent investigations have highlighted the diagnostic potential of UCM in environmental and forensic analyses, but systematic evaluations of mixed-fuel systems are still lacking.[23,24]

In real-world fire, spill, and criminal investigations, petroleum mixtures frequently arise through fuel adulteration, multi-fuel usage, or secondary contamination. Analytical interpretation becomes increasingly difficult when evaporation leads chromatographic patterns to converge toward those of a single fuel type—most commonly diesel—thereby increasing the risk of misclassification. These challenges highlight the importance of robust auxiliary indicators capable of retaining diagnostic information after substantial evaporative loss.

UCM-based indicators offer significant promise because they reflect the collective behavior of broad,

unresolved hydrocarbon fractions rather than relying solely on discrete biomarker peaks. Parameters such as T_{UCM}, hump width (w), and UCM area distribution may provide more stable signatures that remain interpretable even in weathered or mixed samples, complementing traditional GC–MS and pattern-matching approaches.

This study specifically investigates whether UCM-based gas chromatographic profiling can quantitatively distinguish compositional transitions in kerosene–diesel mixtures during evaporation-driven weathering across different mixing ratios. To address this research question, artificially contaminated soil samples with various kerosene–diesel ratios were prepared and subjected to controlled evaporation over a 90-day period, during which GC-based UCM indicators were analyzed to track changes in composition. Unlike previous UCM studies that focused primarily on single-fuel systems, the present work examines mixed petroleum matrices and evaluates how UCM parameters respond to evaporation-induced compositional evolution under controlled laboratory conditions. As a short-term preliminary assessment, this study aims to determine the feasibility and diagnostic value of UCM-based GC profiling for mixed-fuel scenarios and to provide foundational data that can support more reliable forensic interpretation of weathered petroleum mixtures. The findings are expected to contribute to improved analytical frameworks for environmental pollution assessment and to facilitate future database construction for mixed-fuel oil-spill investigations.

2. Material and Methods

2.1. Material and sample preparation

In this study, weathering refers exclusively to evaporation-driven mass loss under controlled laboratory conditions; biodegradation and photodegradation were not examined and are positioned as future research directions. Commercially available kerosene and diesel were used to prepare mixed-fuel samples at ratios of 9:1, 5:1, 4:1, 3:1, 2:1, 1:1, and 1:9 (kerosene:diesel).

To isolate the effects of evaporation from other weathering processes, standard sand (ISO standard sand, EN 196-1) was employed as the soil matrix. Artificially contaminated soil was prepared by adding 0.1 g of the oil mixture to 10 g of standard sand in a 50-mL glass vial. Prior to contamination, the sand was baked at 100 °C for one hour to minimize microbial activity and thereby suppress biodegradation. In addition, the contaminated vials were stored in shaded conditions throughout the experiment to reduce photochemical oxidation and ensure that evaporative loss remained the dominant weathering mechanism. The temperature and relative humidity within the chamber were maintained at approximately 25 °C and 35 %, respectively. All experiments were performed in triplicate (n = 3) to ensure reproducibility of the results.

2.2. Analytical methods

The contaminated soil samples with oil mixtures of varying mixing ratios were eluted with a solvent at the time points of 0, 20, and 90 days. Thereafter, these samples were subjected to gas chromatography (GC) analysis. To execute the GC analysis of the artificially contaminated soil samples, 10 mL of dichloromethane (DCM) and 100 mg of sodium sulfate (Na_2SO_4) were added to the prepared samples. The samples were then stirred at 40 rpm for 30 minutes using a rotary shaker. The impurities were filtered out using a 0.45 μm PTFE filter (Cat. No. 6784-1304; Whatman, UK). The filtered solution was diluted to the appropriate concentration for GC analysis.

The analysis of the prepared samples was conducted using a gas chromatograph (GC-FID, HP 6890N; Agilent Technologies, CA, USA) equipped with a flame ionization detector and an autosampler (7683; Agilent Technologies). A DB-5 capillary column (30 m length × 0.32 mm inner diameter, 0.5 μm film thickness, 19091J-113; Agilent Technologies) was utilized, with nitrogen (N_2) as the carrier gas at a flow rate of 1.0 mL/min. The split ratio was maintained at 1:15. The injector and detector temperatures were set to 300 °C and 320 °C, respectively. For

the oven temperature program, it was initially held at 50 °C for 2 min, followed by a ramp-up at a rate of 8 °C/min to 320 °C, where it was maintained for 20 min.

2.3. Quantification of UCM indicators in the target oil types

To quantify the UCM information of the target oil type, the analytical method reported by Jeon (2017) was adopted with modifications. Briefly, the coordinates of the UCM hump were extracted from the GC chromatograms of each sample, and the UCM indicators were characterized by fitting the hump to a Gaussian function. Gaussian curve fitting was performed using Origin 7.5 software (OriginLab, Northampton, MA, USA) after baseline correction between the retention times of n-octane (C_8) and n-tricosane (C_{23}). The integration limits were defined by the UCM envelope to ensure consistent area quantification across samples.

From the fitted curve, the time corresponding to the maximum point (T_{UCM}) and the width (w) of the UCM hump were obtained as characteristic parameters. In addition, the UCM area (A) derived from the Gaussian fitting was calculated for each fuel type (A1 for kerosene and A_2 for diesel), and the relative area ratio (A_1/A_{1+2} or A_2/A_{1+2}) was used to compare the volatility between fuels (*Fig.* 1). For the triplicate analyses, the relative area ratios were reported as mean ± standard deviation to represent analytical reproducibility.

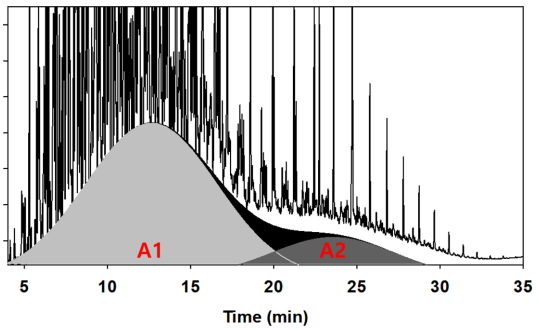

Fig. 1. Enlarged view of the UCM in the GC chromatogram for mixed oil, highlighting the characterized UCM regions: A1 (kerosene) and A2 (diesel).

3. Results and Discussion

3.1. GC-chromatogram and characteristic of UCM

To establish a baseline for evaluating temporal changes in kerosene and diesel content within soil, the UCM characteristics of unweathered contaminated samples (day 0) were initially characterized. Following the extraction of the Gaussian-fitted UCM areas corresponding to each fuel type (A1 for kerosene and A2 for diesel), the relative area ratios were calculated by normalizing each value to the total UCM area (i.e., the sum of A1 and A2) (*Fig.* 1). The analysis showed that the total UCM (T_{UCM}) value of kerosene and the width (w) were 12.1 ± 0.2 and 9.0 ± 0.1, respectively, with a coefficient of determination (R^2) of 0.985 or higher. For diesel, the T_{UCM} value was measured to be 19.9 ± 0.3 and the width (w) to be 15.7 ± 0.2, with an R^2 of over 0.975 (*Fig.* 2). These results are similar to those of the previous studies[23] and support that the T_{UCM} values for kerosene and diesel are well separated, with minimal overlap.

To ascertain the viability of extracting UCM characteristic indicators for oil mixtures, a GC analysis was conducted on a series of oil mixtures at varying mixture ratios (e.g., 9:1, 5:1, 4:1, 3:1, 2:1, 1:1, 1:9, etc.). The analysis indicated that, even when one of the components in the oil mixture was present in an absolutely dominant proportion (9:1 or 1:9, kerosene: diesel), the characteristics of the two UCM zones (A1 and A2) could be identified (*Fig.* 3). Particularly, previous study also reported that the boundary between the two zones was clearly defined in oil mixtures, which was reconfirmed in this experiment.[23] Under various mixture ratio conditions, the UCM section (A1 and A2) was distinctly delineated, and based on this, the UCM data of oil mixtures could be characterized and utilized for analysis. Conclusively, it was ascertained that the UCM characteristic indicator (T_{UCM}) of kerosene and diesel does not overlap with each other, and that the UCM range of each component can be distinctly distinguished even in mixed oil types. These results can be used as important data for the interpretation of mixed oils and quantitative analysis of

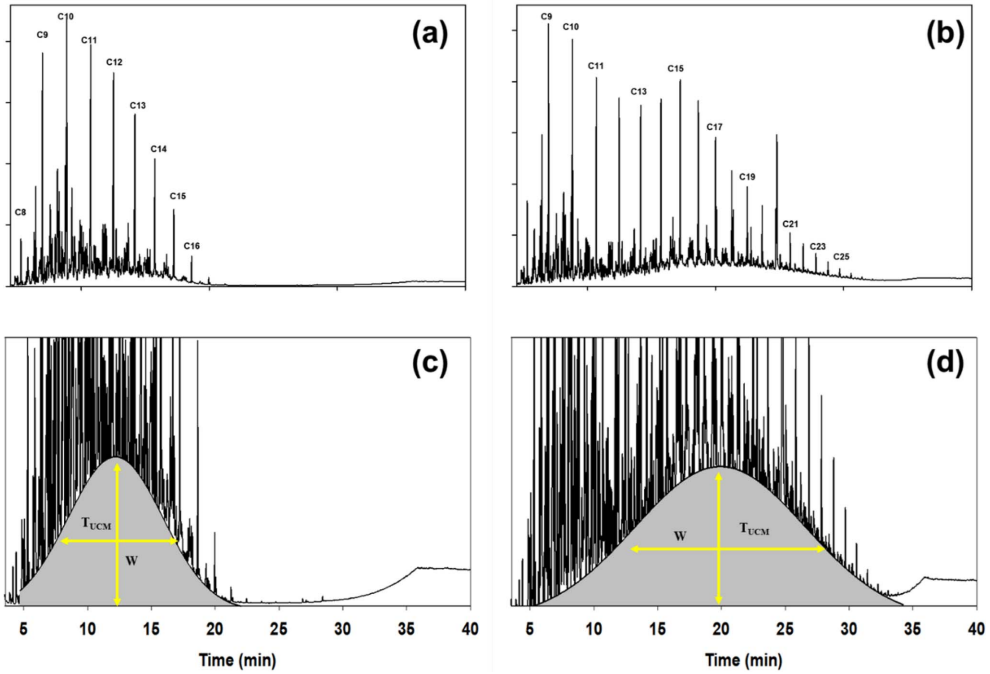

Fig. 2. GC data for kerosene (a) and diesel (b), along with enlarged UCM regions fitted with Gaussian regressions (R^2 > 0.97), showing TUCM and w values for kerosene (c) and diesel (d).

their components.

3.2. Evaporative weathering characteristic of oil mixture according to mixture ratio

We observed the evaporative weathering characteristics of oil in contaminated soil with oil mixtures of various mixture ratios for 0, 20, and 90 days (*Fig.* 4). Experiments indicated that a common pattern of evaporative weathering of low-molecular-weight, low-boiling compounds was observed in all mixture ratios. At the 90-day mark, n-alkanes with a C_{13} or higher were identified as the predominant peaks, and the majority of compounds with a C_{13} or lower were found to have evaporated. This indicated that the evaporative weathering rate of kerosene, which contained a greater proportion of low-boiling compounds, surpassed that of diesel.

The accelerated evaporation rate of kerosene relative to that of diesel can be attributed to the disparity in the chemical composition and physical properties of these two oils. Kerosene is composed primarily of a mixture of light hydrocarbons in the C_{10}–C_{16} range, which possess small molecular sizes and high volatility. As these small molecules are easy to evaporate, they evaporate faster under normal environmental conditions. Conversely, diesel is characterized by a substantial presence of C_{16} or larger hydrocarbons, which possess greater molecular size and mass. This molecular configuration results in reduced volatility and enhanced resistance to evaporation.[25] Furthermore, due to the relatively wide molecular weight distribution of diesel, heavy hydrocarbons persist for an extended duration subsequent to evaporation.[2,7-9] As indicated in extant studies, kerosene exhibits a higher rate of evaporation compared with that of diesel, which aligns with that of the experimental findings.

Summarily, kerosene exhibits a higher evaporation rate under environmental conditions. This phenomenon can be attributed to the relatively small molecular structure and low molecular weight of kerosene. Contrarily, given the elevated proportion of heavy compounds in diesel, its evaporation rate is reduced, and the residual time is extended. This property is

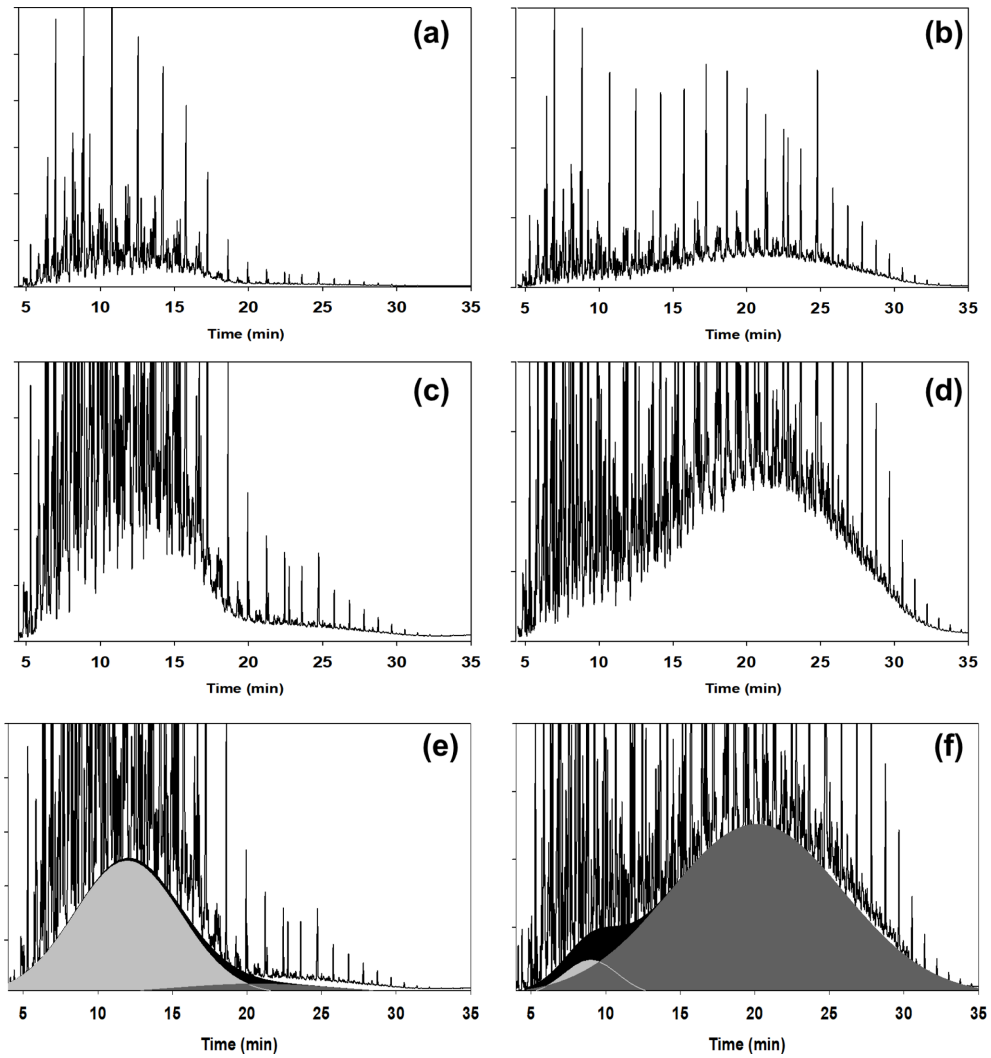

Fig. 3. GC data ((a) and (b)), enlarged UCM regions ((c) and (d)), and characterized UCM areas ((e) and (f)) for mixed oil with extreme mixing ratios of kerosene to diesel: 9:1 (left) and 1:9 (right)

significant in the identification of pollutant characteristics in the environment. Our findings offer valuable insights into the processes of evaporation and evaporative weathering of oil mixtures, thereby facilitating a more comprehensive understanding of environmental pollution.

3.3. UCM characteristic of oil mixture according to mixture ratio

The UCM of oil mixtures with various mixture ratios was observed (*Fig.* 4), followed by the specification of the values (*Fig.* 5) and quantification (*Fig.* 6) for analysis. It was observed that the greater the mixture ratio of kerosene, the greater the area of the UCM of kerosene compared with that of diesel. However, the T_{UCM} values did not differ significantly. As time progresses, it becomes evident that the configuration of the front end of the chromatogram undergoes a collapse, concomitant with the presence of n-alkane, iso-alkane, and the UCM hump. UCM is recognized as a multifaceted amalgamation of over several hundred unidentifiable substances. Earlier studies

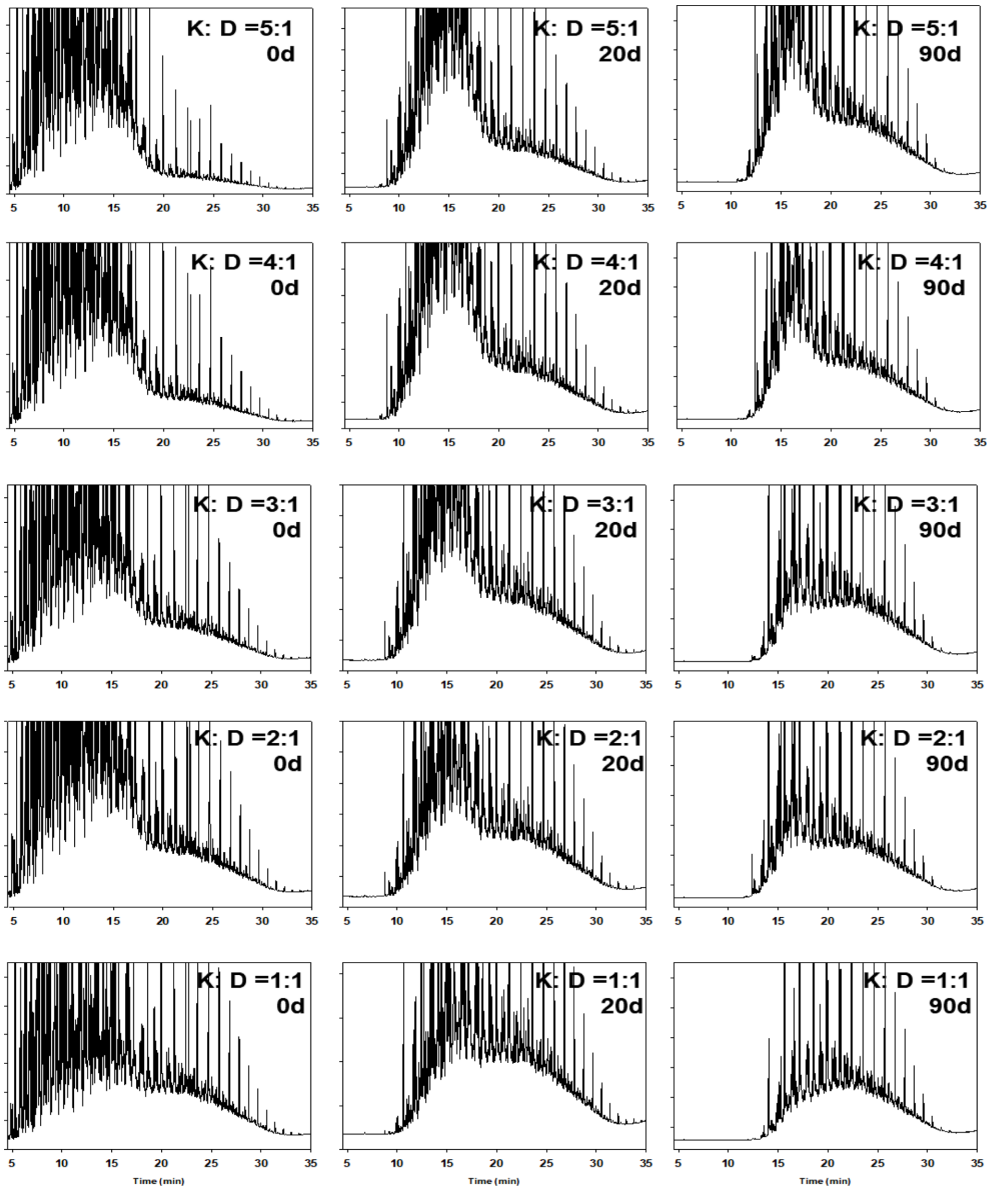

Fig. 4. GC data and enlarged UCM regions for various mixing ratios (5:1, 4:1, 3:1, 2:1, and 1:1) of kerosene (K) to diesel (D) over time (0 days (0d), 20 days (20d), and 90 days (90d)).

indicated that UCM exhibits enhanced weathering resistance in comparison with that of other components within oil.[26,27] This study corroborated that UCM was also susceptible to evaporative weathering, albeit with variations in the extent of evaporative weathering.

Figs. 4 and 5 were designed to visually illustrate how the UCM pattern evolves over time and according to the kerosene–diesel mixing ratio. These figures intentionally present the qualitative chromatographic transformation—such as the collapse of the front-end region, progressive loss of n-alkanes below C_{13}, and changes in the UCM hump—to allow readers to visually grasp the direction and magnitude of compositional shifts prior to quantitative interpretation.

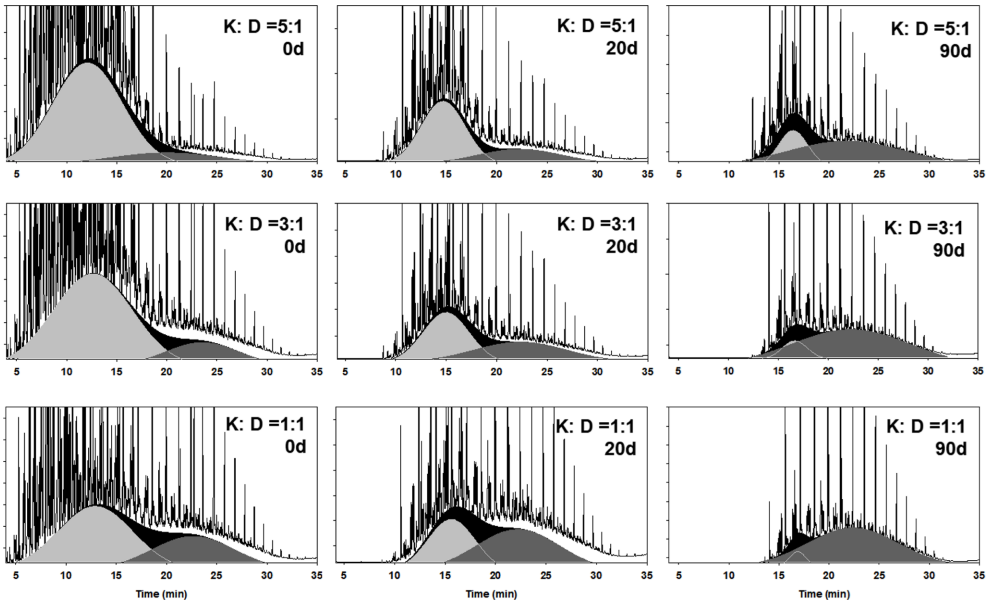

Fig. 5. Characterized UCM regions for various mixing ratios (5:1, 3:1, and 1:1) of kerosene (K) to diesel (D) over time (0 days (0d), 20 days (20d), and 90 days (90d).

Because the purpose of *Figs.* 4 and 5 is to show these visual chromatographic changes rather than numerical comparison, detailed quantification was intentionally reserved for *Fig*. 6.

Figs. 5 and 6 illustrate the UCM characterization and relative area ratios of kerosene–diesel mixtures with varying mixing ratios (5:1, 3:1, and 1:1). As shown, kerosene evaporated more rapidly than diesel, consistent with previous findings that kerosene contains a higher proportion of low-boiling, low-molecular-weight hydrocarbons that volatilize quickly. The qualitative evidence presented in *Figs.* 4 and 5 is further supported by the quantitative evaluation in *Fig.* 6, which enables clearer interpretation of mixture-dependent evaporative behavior. The UCM values of the mixtures were quantified to further elucidate these compositional changes.

Under the 5:1 (kerosene:diesel) condition, the relative UCM area ratio was initially 0.85 ± 0.03 for kerosene and 0.15 ± 0.03 for diesel. These ratios changed to 0.68 ± 0.02 and 0.32 ± 0.02 after 20 days, and to 0.46 ± 0.03 and 0.53 ± 0.03 after 90 days. When the mixing ratio was 3:1, the initial values of 0.81 ± 0.02 and 0.19 ± 0.02 shifted to 0.39 ± 0.02 and 0.61 ± 0.01 after 90 days. In contrast, when the ratio was 1:1, the variation in UCM area ratio was relatively small compared with that of other mixtures (*Fig.* 6). These results support that kerosene exhibits a higher evaporation rate than diesel, as evidenced by the progressive changes in the UCM area ratio. The volatility behavior of kerosene depended strongly on the mixing ratio, and this trend became more pronounced over time. After 90 days, despite substantial compositional changes, the UCM area ratio of diesel exceeded twice that of kerosene, indicating differential volatilization rates between the two components.

Although each experiment was conducted in triplicate (n = 3), the results showed high reproducibility (R^2 > 0.97) across replicates. The error bars are presented in *Fig.* 6 to indicate the analytical consistency and reliability of the measurements. While formal calibration and inter-method validation were not performed in this feasibility-oriented study, the high reproducibility (R^2 > 0.97) supports the reliability of the analytical approach. This work aimed to indicate the applicability of UCM-based GC profiling to mixed and weathered oil samples rather than to establish a fully calibrated quantitative model. Future research will incorporate

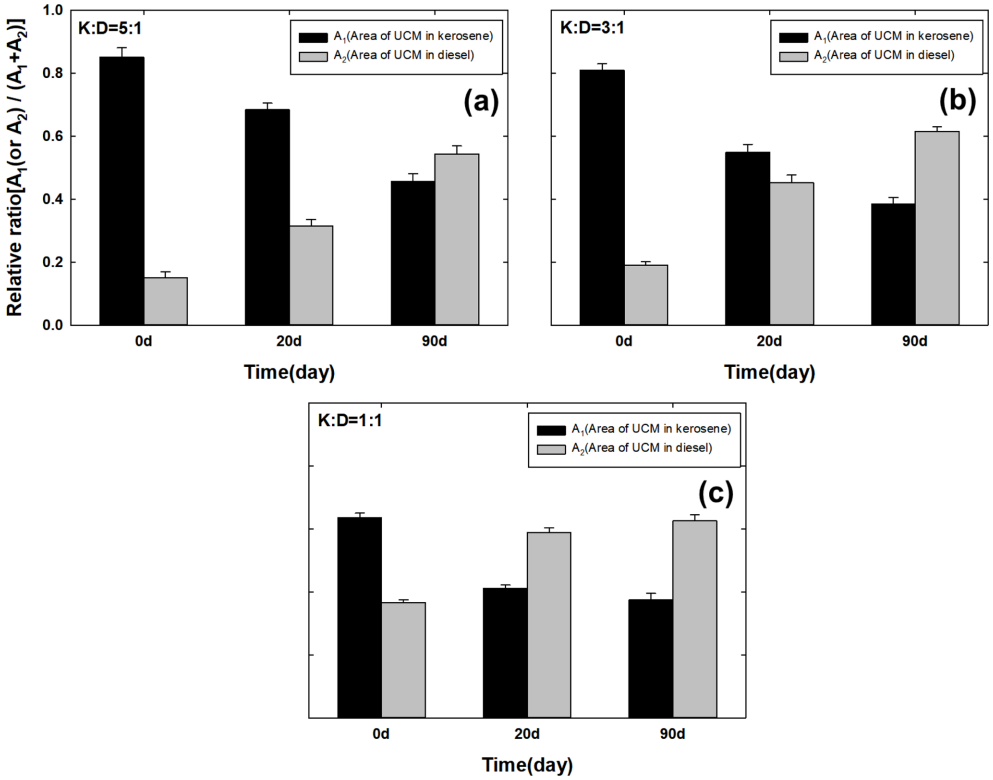

Fig. 6. Relative area ratios (A1 and A2) for various mixing ratios (5:1(a), 3:1(b), and 1:1(c)) of kerosene (K) to diesel (D) over time (0 days (0d), 20 days (20d), and 90 days (90d)). Error bars represent ±1 standard deviation (n = 3). The results showed high consistency among triplicate runs ($R^2 > 0.97$).

quantitative calibration using certified reference standards and GC–MS validation to enhance the robustness and traceability of the method.

Overall, *Figs.* 4 and 5 provide essential visual context for understanding how the chromatographic profile evolves under different mixing ratios and time conditions, while *Fig.* 6 delivers the detailed quantitative evidence necessary to interpret these visual patterns more rigorously. Together, these figures offer a complementary framework that strengthens the analytical depth of the study.

3.4. Usefulness of data interpretation using UCM characteristic indicators

This study evaluated the evaporative weathering behavior of kerosene–diesel mixtures using UCM-based interpretation. Consistent with previous findings, the quantitative results supported that low-boiling and low-molecular-weight hydrocarbons volatilize first and that kerosene exhibits a faster evaporation rate than diesel, particularly at higher mixing ratios. These outcomes indicate that UCM-derived metrics provide meaningful insight into compositional transitions of mixed fuels during short-term evaporation.

Figs. 4–6 collectively illustrate how chromatographic patterns and UCM values evolve under weathering. *Figs.* 4 and 5 show the qualitative disappearance of front-end peaks, including the loss of C_8–C_{12} hydrocarbons, while *Fig.* 6 provides quantitative evidence through relative UCM area ratios corresponding to these visual changes.

As shown in *Fig.* 7(a), kerosene and diesel share many overlapping compounds. After extensive evaporation, the loss of low-boiling hydrocarbons causes the front region of the chromatogram to collapse, resulting in profiles that resemble diesel.

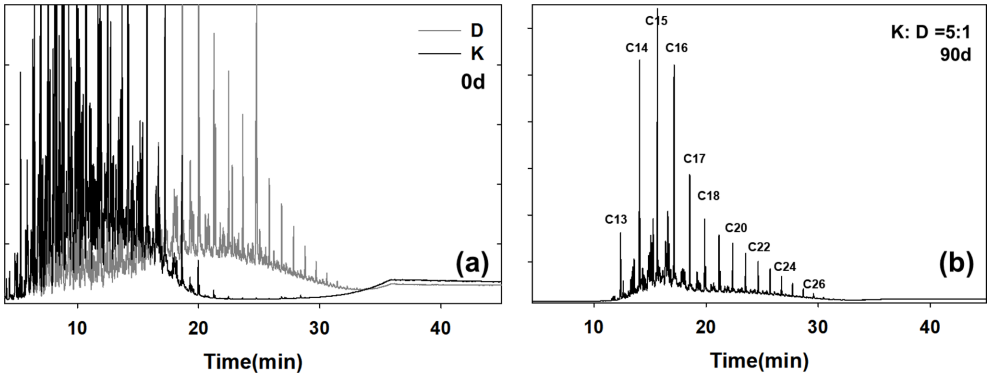

Fig. 7. GC overlapping data of kerosene and diesel(a) for 0 days, and GC data of oil mixture (K:D=5:1) over 90 days.

This visual convergence makes it difficult to determine whether a weathered sample originated from a mixture or a single fuel based only on peak patterns. *Fig.* 7(b) indicates that after 90 days of evaporation, hydrocarbons in the C_{13}–C_{23} range dominate the chromatogram, yielding a pattern similar to diesel despite the mixture initially containing a fivefold excess of kerosene.

Such convergence introduces the risk of misinterpretation in forensic assessments, as kerosene may become visually undetectable even when originally present at high proportions. This limitation underscores the need for complementary indicators that remain interpretable after extensive evaporative loss.

UCM-based indicators address this need by providing a stable distributional signature that persists beyond the disappearance of individual peaks. Parameters such as relative UCM area ratio, peak width, and TUCM allow the analyst to detect the presence of mixed oils and assess the extent of evaporation even when the chromatogram resembles a single fuel type. Thus, UCM-based interpretation serves as a robust auxiliary tool within the range examined here for distinguishing weathered mixtures and enhances the reliability of forensic evaluations.

4. Conclusions

This study investigated the evaporative behavior of kerosene, diesel, and their mixtures using gas chromatography and Unresolved Complex Mixture (UCM) indicators. The results indicated that the UCM parameters—particularly T_{UCM} and peak width (w)—effectively distinguished between kerosene and diesel, even in blended and weathered samples. These parameters provided a useful basis for both qualitative and quantitative interpretation of oil mixtures that had undergone evaporation. The evaporation rate of kerosene was consistently higher than that of diesel, reflecting its higher proportion of low-boiling and low-molecular-weight compounds. As evaporation progressed, the UCM area decreased more rapidly in samples with higher initial kerosene content, while compounds above C_{13} became dominant after 90 days.

It should be noted that the present work represents short-term laboratory evaporation experiments rather than long-term environmental weathering. Nevertheless, the results support the feasibility of applying UCM-based GC profiling to evaluate the early-stage compositional evolution of mixed oils and to improve the interpretation of weathered petroleum samples.

UCM was reaffirmed as a valuable complementary indicator for distinguishing mixed and weathered oil samples. Even when typical chromatographic peaks are diminished or obscured by evaporation, UCM profiling enables the indirect identification of blended oils through a comprehensive analysis of distributional characteristics.

Although limited in duration, this study establishes a methodological foundation for forensic and environmental applications of UCM analysis. Future research will extend this approach through long-term

weathering experiments and analyses of low-concentration oil mixtures, thereby enhancing the precision and applicability of UCM-based diagnostics in environmental forensics.

Acknowledgements

This work was supported by National Forensic Service (NFS2026CHE01), Ministry of the Interior and Safety, Republic of Korea.

Declaration of Competing Interest

The authors declare that there is no conflict of interest.

References

1. R. Borusiewicz, G. Zadora, and J. Zieba-Palus, *Chromatographia*, **60**(Suppl 1), S133-S142 (2004). https://doi.org/10.1365/s10337-004-0299-4
2. A. M. Hupp, L. J. Marshall, D. I. Campbell, R. W. Smith, and V. L. McGuffin, *Anal. Chim. Acta*, **606**(2), 159-171 (2008). https://doi.org/10.1016/j.aca.2007.11.007
3. G. L. Alexandrino, J. Malmborg, F. Augusto, and J. H. Christensen, *J. Chromatogr. A*, **1591**, 155-161 (2019). https://doi.org/10.1016/j.chroma.2019.01.042
4. C. Yang, Z. D. Wang, B. Hollebone, C. E. Brown, M. Landriault, B. Fieldhouse, Z.Y. Yang, *Environ. Forensics*, **13**(4), 298-311 (2012). https://doi.org/10.1080/15275922.2012.730114
5. Y. Sun, J. Guan, G. Yue, Y. Xiu, H. Wang, T. McHugh, and J. Ma, *Environ. Forensics*, **26**(4), 485-500 (2025). https://doi.org/10.1080/15275922.2025.2459405
6. I. R. Kaplan, Y. Galperin, S. T. Lu, and R. P. Lee, *Org. Geochem.*, **27**(5-6), 289-299, 301-317 (1997). https://doi.org/10.1016/S0146-6380(97)87941-7
7. F. Ahmed and A. N. M. Fakhruddin, *Int. J. Environ. Sci. Nat. Resour.*, **11**(3), 1-7 (2018). https://doi.org/10.19080/IJESNR.2018.11.555811
8. B. P. Vempatapu and P. K. Kanaujia, *Trends Anal. Chem.*, **92**, 1-11 (2017). https://doi.org/10.1016/j.trac.2017.04.011
9. B. P. Vempatapu, D. Tripathi, J. Kumar, and P. K. Kanaujia, *SN Appl. Sci.*, **1**, 614 (2019). https://doi.org/10.1007/s42452-019-0637-7
10. T. A. Knoerzer, E. M. Hill, T. A. Davis, S. T. Iacono, J. E. Johnson, and G. J. Balaich, *J. Chem. Educ.*, **95**(10), 1821-1826 (2018). https://doi.org/10.1021/acs.jchemed.8b00216
11. M. A. Tarr, P. Zito, E. B. Overton, G. M. Olson, P. L. Adhikari, and C. M. Reddy, *Oceanography*, **29**(3), 126-135 (2016). https://doi.org/10.5670/oceanog.2016.77
12. A. M. de Oliveira, J. E. B. Castiblanco, F. P. Fleming, E. N. R. de Souza, and L. W. Hantao, *Energy & Fuels*, **34**(9), 10705-10712 (2020). https://doi.org/10.1021/acs.energyfuels.0c01613
13. R. W. Smith, R. J. Brehe, J. W. McIlroy, and V. L. McGuffin, *Forensic Chem.*, **2**, 37-45 (2016). https://doi.org/10.1016/j.forc.2016.08.005
14. M. A. Gough and S. J. Rowland, *Nature*, **344**, 648-650 (1990). https://doi.org/10.1038/344648a0
15. G. S. Frysinger, R. B. Gaines, L. Xu, and C. M. Reddy, *Environ. Sci. Technol.*, **37**(8), 1653-1662 (2003). https://doi.org/10.1021/es020742n
16. P. A. Sutton, C. A. Lewis, and S. J. Rowland, *Org. Geochem.*, **36**(6), 963-970 (2005). https://doi.org/10.1016/j.orggeochem.2004.11.007
17. G. T. Ventura, F. Kenig, C. M. Reddy, G. S. Frysinger, R. K. Nelson, and B. Van Mooy, R. B. Baines, *Org. Geochem.*, **39**(7), 846-867 (2008). https://doi.org/10.1016/j.orggeochem.2008.03.006
18. A. A. Elfadly, O. E. Ahmed, and M. M. El Nady, *Egypt. J. Pet.*, **26**(4), 969-979 (2017). https://doi.org/10.1016/j.ejpe.2016.11.007
19. G. Dević, S. Bulatović, J. Avdalović, N. Marić, J. Milić, M. Ilić, and T. Šolević Knudsen, *Molecules*, **30**(1), 154 (2025). https://doi.org/10.3390/molecules30010154
20. L. Asia, S. Mazouz, M. Guiliano, P. Doumenq, and G. Mille, *Mar. Pollut. Bull.*, **58**(3), 443-451 (2009). https://doi.org/10.1016/j.marpolbul.2008.11.022
21. Z. Wang, S. A. Stout, and M. Fingas, *Environ. Forensics*, 7(2), 105-146 (2006). https://doi.org/10.1080/15275920600667104
22. K. Ramadass, S. Kuppusamy, K. Venkateswarlu, R. Naidu, and M. Megharaj, *Crit. Rev. Environ. Sci. Technol.*, **51**(23), 2872-2894 (2021). https://doi.org/10.1080/10643389.2020.1813066
23. S. K. Jeon, D. Kwon, and S. Lee, *Sci. Total Environ.*, **607-608**, 42-52 (2017). https://doi.org/10.1016/j.scitotenv.

2017.06.251
24. L. L. Martins, V. B. Pereira, A. P. Nascimento, R. N. A. Azevedo, A. H. Oliveira, C. E. P. Teixeira, D.A . Azevedo, G. F. da Cruz, R. M. Cavalcante, T. Giarrizzo, *Environ. Sci. Technol.*, **58**(21), 9328-9338 (2024). https://doi.org/10.1021/acs.est.4c01520
25. M. M. Elkotb, S. L. Aly, and H. A. Elsalmawy, *Combust. Flame*, **85**(3-4), 300-308 (1991). https://doi.org/10.1016/0010-2180(91)90135-X
26. I. M. Head, D. M. Jones, and S. R. Larter, *Nature*, **426**, 344-352 (2003). https://doi.org/10.1038/nature02134
27. C. Hallmann, L. Schwark, and K. Grice, *Nat. Geosci.*, **1**, 588-591 (2008). https://doi.org/10.1038/ngeo260